Annex J – RANDO SOLUTION'S FINAL REPORT

Note: This Annex appears in its original format.

AVT-308 UQ Final Report

Introduction

For efficient coalition mission planning of NATO forces under different terrain scenarios and for selection of capable vehicles, reliability-based stochastic off-road mobility maps are developed. Traditionally, the analysis considers nominal deterministic values of key variables involved in the terrain properties and terramechanics simulation model. The generated deterministic mobility maps could be around 50% reliable and thus cannot be used effectively in mission planning of NATO forces under different terrain scenarios and for selection of capable next generation combat vehicles. Thus, it is desirable to develop reliability-based stochastic mobility maps (i.e., Speed-Made-Good and GO/NOGO) that can provide desirable reliability levels in determining mobility of military vehicles across various terrains.

Key variables of off-road conditions include those related to terrain elevation data and soil property data as shown in Fig. 1 [1]. The ground vehicle parameters and their variabilities could also be addressed for a full stochastics treatment, but were not considered in this study. The terrain elevation data are usually obtained using remote sensory techniques (i.e., radar technology, imagery methods, etc.). Those techniques lead to uncertainty in terrain data values as well as the spatial position of data points. Thus, any elevation model of the terrain includes uncertainty. Digital Elevation Models (DEMs) produced by the US Geological Survey agency are a good example of this issue. Spatial variability of physical terrain properties (e.g. soil bulk density, cohesion, internal friction angle, Bekker-Wong parameters, etc.) also leads to uncertainty in vehicle-terrain interaction models. In addition, measurement methods of the soil properties are uncertain in nature.

The current NRMM output is given in terms of a deterministic mobility map [2, 3]. This map shows the means of cross-country speed between two points in a given region for a given vehicle. As recommended by Refs. 4 and 5, a stochastic analysis should be carried out in terms of probability densities and reliabilities. However, previous attempts to convert NRMM from a deterministic framework to a stochastic one have failed in the origin of uncertainties. No formal mathematical reasoning about the uncertainty types that need to be introduced in the simulations was given in Refs. [4, 5, 6]. Also, the current NRMM does not support autonomous mobility (this issue was pointed out in Ref. [7]). While this capability is highly desirable in the NG-NRMM because current and future defense forces include autonomous systems, it was not considered by Thrust Area 5.

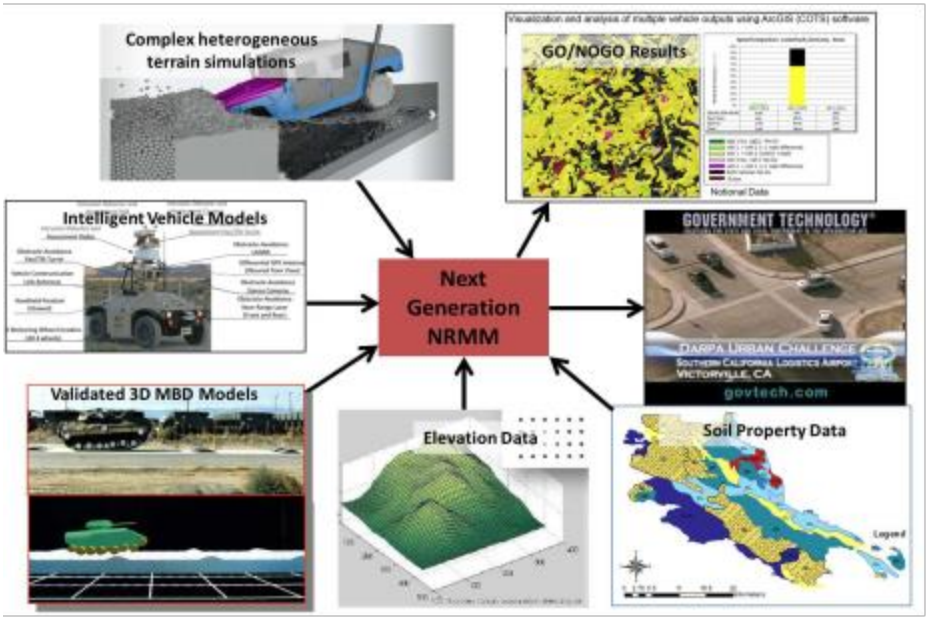

Fig. 1: NG-NRMM Mobility Map Generation [1]

Uncertainty quantification (UQ) was carried out for speed made good for the AVT-308 CDT event. This work was carried out in collaboration with the software vendors and KRC. The stochastic map for each vendor's terramechanics vehicle was generated following the UQ framework for generation of stochastic mobility maps as defined in Chapter 6 of the AVT-248 final report. The reader is referred to that report for details on the UQ framework and process.

Elevation and Slope Input Variability

The variability in elevation was provided by KRC and there were two different resolutions for elevation variability, one for ±9 m and the other for ±3 cm. Fig. 2 below shows the map that defines the elevation variability for the high- and low-resolution areas. The elevation variability was assumed to have a normal distribution with the mean set as the measured elevation and the standard deviation set to match the ±9m or ±3cm depending on the geospatial location. Using the elevation variability, a 1000 elevation realization rasters were generated. ArcGIS was then used to calculate the corresponding slope for each of the 1000 elevation realization rasters. The slope variability is shown in the maps below in Fig. 2. The 90% slope means there is 90% probability that the maximum slope is less than or equal to the slope value shown in the map.

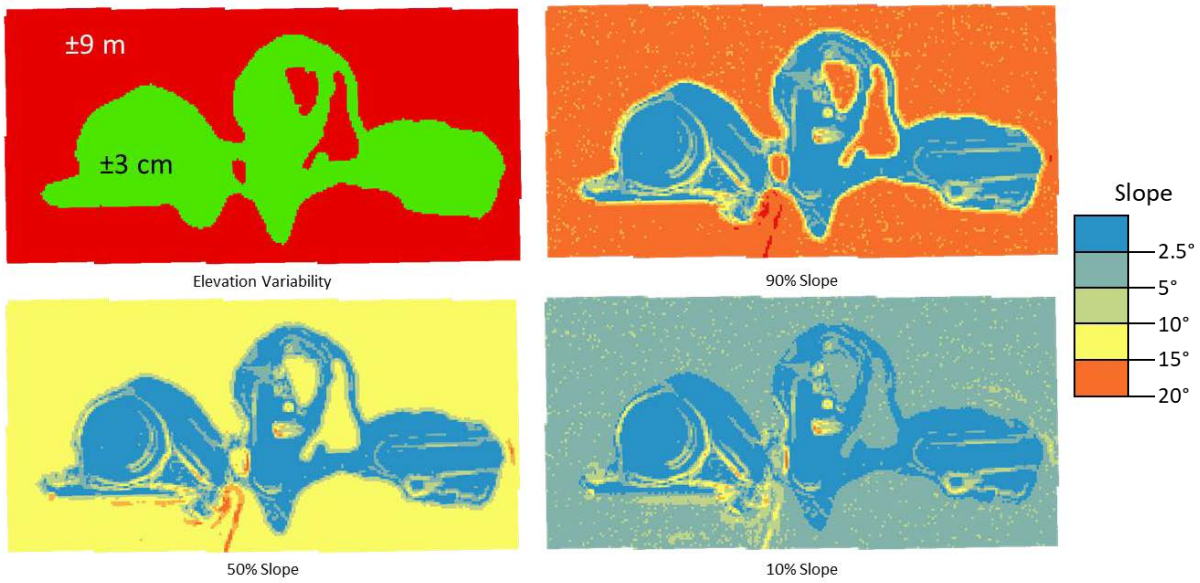

Fig. 2: Elevation and Slope Variability

The KRC collected soil data using the bevameter and laboratory testing, the reader is referred to the AVT-308 final report KRC portion for details on the testing conducted. The soil parameter properties were available for each of the five soil types at KRC.

Simple Terramechanics Input Variability

For simple terramechanics the Bekker-Wong parameters, obtained from the bevameter testing data, were used as the input soil parameters for the simple terramechanics simulations. The number of measurements for each soil type and property varied anywhere from four to nine as shown in Table 1 below. These data were then used to determine one of the standard distribution types that best fits the data. During the fitting process it was assumed all soil properties were independent, i.e., not statistically correlated with each other. That assumption was made because the number of data was so few, four to nine points, that it was not meaningful to determine any statistical correlation. That is, the process would be difficult and not straight forward being the number of data was so few.

Table 1: Soil Type and Number of Data

Soil Type	Number of Data
2NS Sand	8
Coarse Pit	6
Fine Grain Pit	9
Rink Natural	4
Stability	4

Once the distribution types to be used for each soil parameter and soil type were determined, the design of experiment (DOE) points were generated. The DOE points were generated using RAMDO software dynamic Kriging (DKG) fitting process. The RAMDO DKG fitting process generated DOE points in the variance window, i.e., the domain defined the variability of the soil parameters. The generated DOE

points were then provided to the software vendors for them to carry out vehicle dynamic analysis and return the speed made good.

These DOE points raised several questions and issues from the vendors. One issue raised was that the Kc and Kphi values for some of the DOE points were negative. The vendors were not able to run the DOE points that negative values for Kc and Kphi. In order to overcome this difficulty, it was proposed by one vendor, Dr. Wong, to use Keq instead of Kc and Kphi. [REFERENCE to Dr. Wong's report – writeup on what to do with negative parameters] The KRC then took the original bevameter data gathered and calculated Keq for all the measurements. The second issue raised was that some of the DOE points for the Keq and n parameters seemed to create a soil type that was not physically meaningful, e.g., a soil that is as firm as concrete or even firmer. It was determined that this happened for two reasons. The first was that it was assumed the soil parameters were independent, when in fact there should be some statistical correlation between the parameters. The second, was that the number of data points for each soil type was so few, the distributions fitted to these data points were probably wider than the true variability.

In order to try to overcome this issue it was decided that some of the KRC soil types be grouped together and treated as one soil type in order to assemble a larger data set for a given soil type. This grouping also allowed data from Ref. [8] to be aggregated with the KRC data to create a larger data set. The grouping of the soil types and number of data for group is shown in Table 2 below.

Table 2: Soil Groups and Number of Data

Soil Type	Soil Group	Number of Data
2NS Sand	Sand	20
Coarse Pit		
Fine Grain Pit	Silt	9
Rink Natural	Sandy Loam	18
Stability		
Peat	Peat	N/A

Using the larger data sets the fitting of known distributions for each parameter was done. The distributions that best fit each soil parameter for each soil group are shown in Table 3. During the fitting it was noticed that the fitting of most of the distributions were similar with some having wider tails than others. This would be expected because the number of data used for fitting the distributions was small. Using the larger data sets for the soil groups the statistical correlation between Keq and n was studied and the best fitting copula type and the corresponding Kendall's tau for the correlation are shown in Table 4. Fig. 3 and Fig. 4 show the contour plots of the joint distributions for Keq and n for sand and silt, the data used for fitting the joint distribution is shown as well. Studying Fig. 3 it is seen that the 2-sigma contour of the joint distributions captures almost all of the 20 data points used to fit the distribution and identify the copula type. However, the joint distribution covers the area shown by the green 4-sigma contour in the plot. This raises the question if the distribution is too wide and if the true underlying joint distribution would cover an area much closer to the area covered by the 2-sigma contour shown in the plot. In order to better fit the true distribution to see this, more data points would be needed. The same question arises when studying the joint distribution for Keq and n for silt shown in Fig. 4.

Table 3: B.W. Soil Parameter Distribution Types

Soil Group	nAvg for Keq	Keq	C Grouser	Phi Grouser	Kavg Grouser	C Rubber	Phi Rubber	Kavg Rubber
Sand	Weibull	Gamma	Weibull	Normal	Gamma	Exponential	Normal	Gamma
Sandy Loam	Lognormal	Exponential	Weibull	Weibull	Gamma	Exponential	Weibull	Gamma
Silt	Weibull	Exponential	Weibull	Weibull	Gamma	Exponential	Weibull	Gamma
Peat	Weibull	Exponential	Weibull	Weibull	Gamma	Exponential	Weibull	Gamma

Table 4: Identified Copula Type

Soil Group	Copula Type	Kendall's Tau
Sand	Frank	0.37
Sandy Loam	A14	0.68
Silt	Gumbel	0.6

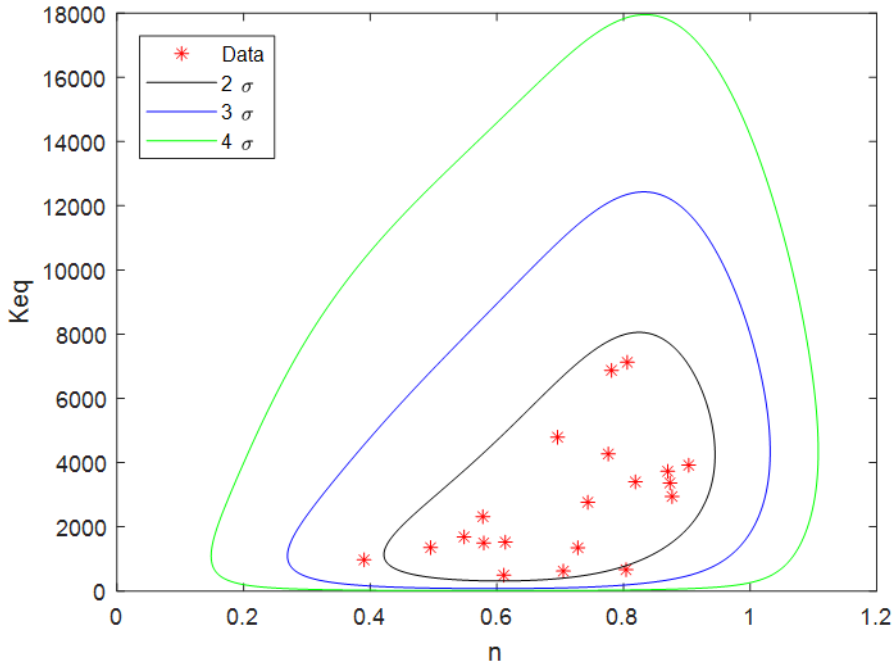

Fig. 3: Joint Distribution Contours for Sand

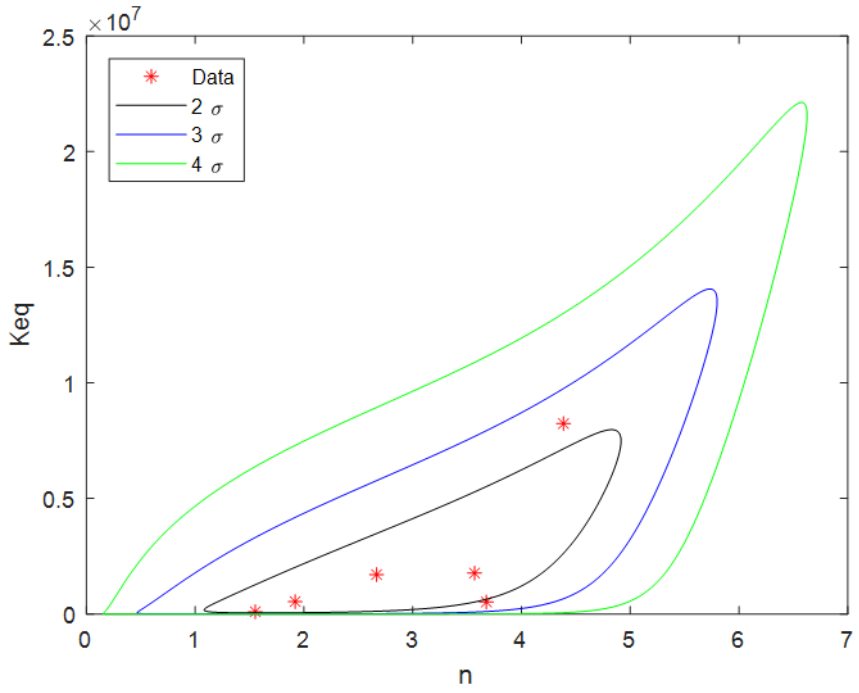

Fig. 4: Joint Distribution Contours for Silt

Using the newly identified distributions, new DOE points were generated. The software vendors seemed to believe these new DOE points represented real-world physical soils more closely, but there were still a few points that might be questionable. However, without having more data to fit a distribution that is much closer to the true distribution, it is not possible to generate better DOE points. The number of data points needed to try to fit a distribution that is much closer to the true distribution is unknown. It really depends on how complex the distribution is, the number of points needed might range anywhere from fifty, to several hundred or even several thousand. The new DOE points were evaluated by the software vendors. The software vendors supplied the calculated speed made good for the new DOE points. The dynamic Kirging (DKG) model for each soil group, for each vendor was created. Using the sequential sampling process in RAMDO additional DOE points were generated, evaluated by the vendors and speed made good results used to refine the DKG model to improve the accuracy of the DKG model.

Complex Terramechanics Input Variability

For the complex terramechanics simulation, the input soil parameters used were not the Bekker-Wong parameters, but were slope, friction angle (Phi), cohesion (C), and bulk density. The slope variability was the same as previously described. For the complex terramechanics the original five soil types shown in Table 1 were used. The complex terramechanics vendor analyzed the laboratory testing data provided by KRC for the friction angle, cohesion, and bulk density in detail. From their experience they provided what they thought were reasonable lower and upper bounds for the variability of the three parameters, as well as what they thought the mean value was for the three parameters. A generalized extreme value distribution was fitted for each soil type using the provided information. Fig. 5 – Fig. 9 show the distributions fitted for the friction angle phi, cohesion C, and bulk density for each of the five soil types. It was assumed that all the parameters are statistically independent. The DOE points for complex

terramechanics were then generated and provided to the vendor for evaluation. The DKG model was created using the provided speed made good results.

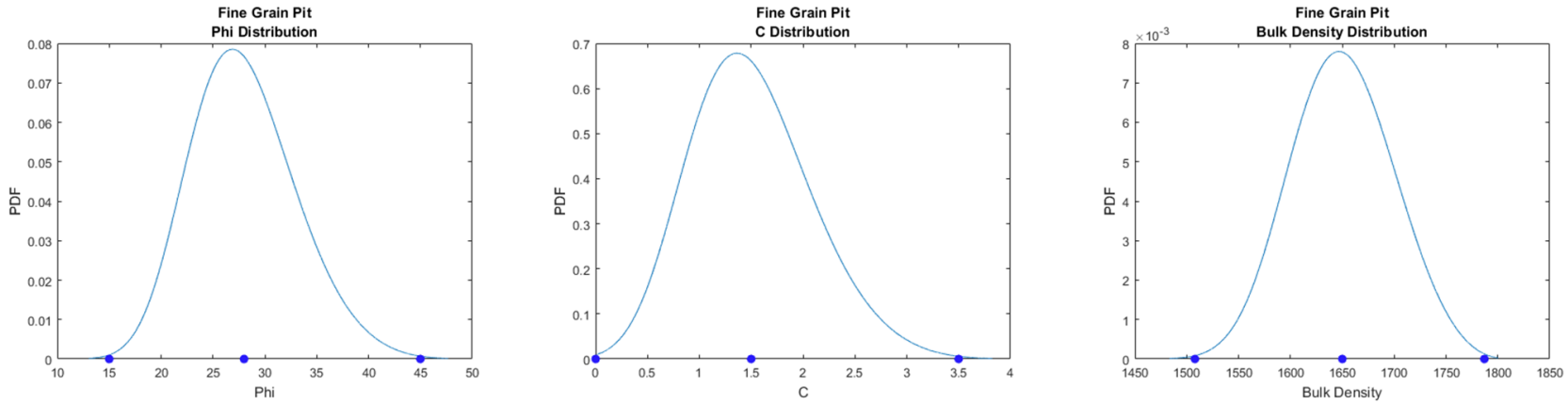

Fig. 5: Fine Grain Pit Distributions for Phi, C, and Bulk Density

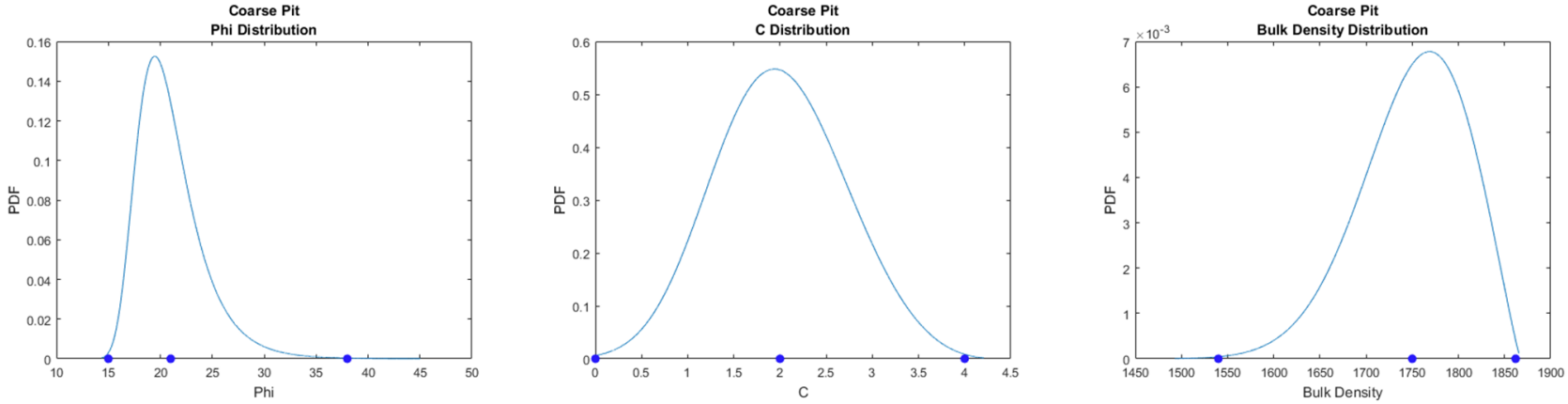

Fig. 6: Coarse Pit Distributions for Phi, C, and Bulk Density

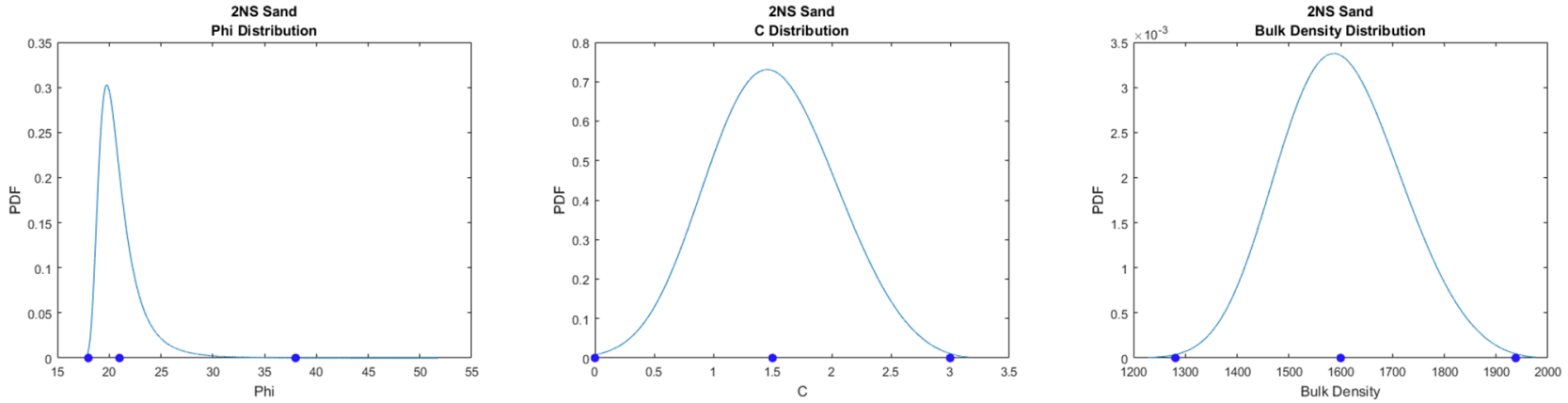

Fig. 7: 2NS Sand Distributions for Phi, C, and Bulk Density

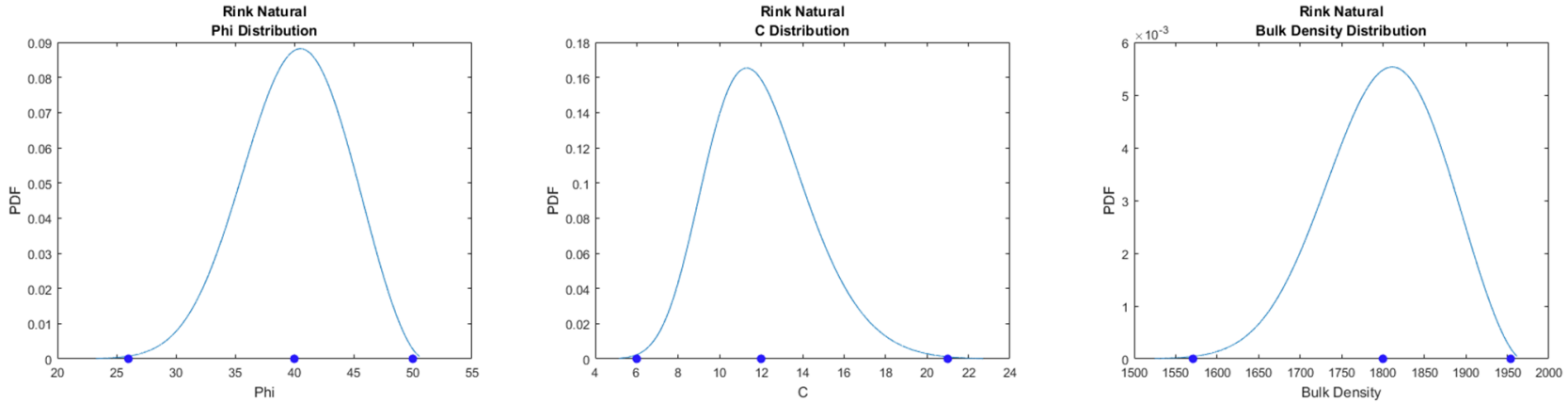

Fig. 8: Rink Natural Distributions for Phi, C, and Bulk Density

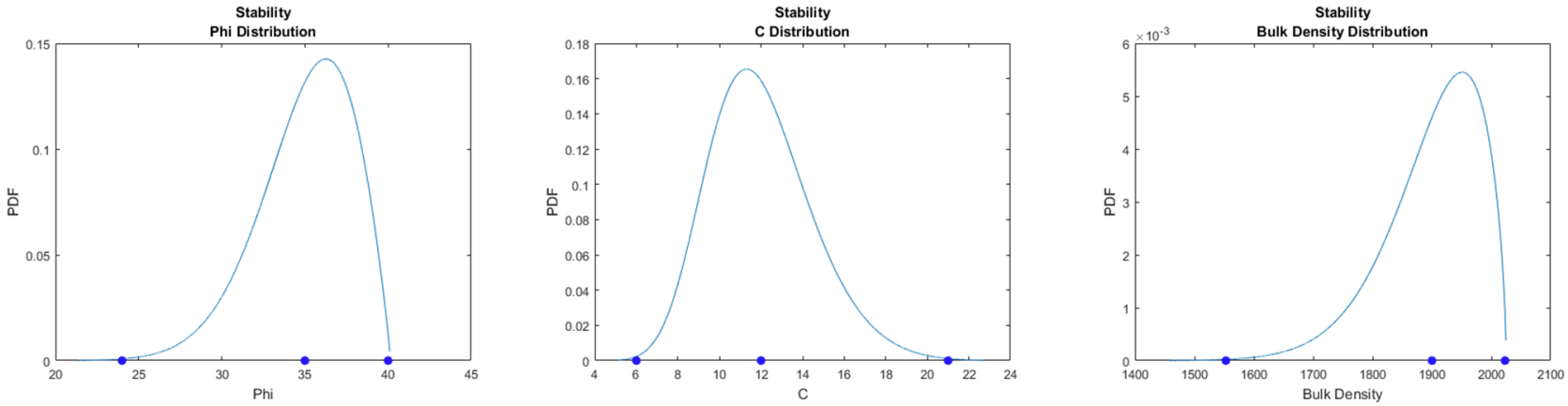

Fig. 9: Stability Distributions for Phi, C, and Bulk Density

Uncertainty Quantification of Speed Made Good

After fitting the DKG models for both the simple and complex terramechanics methods, uncertainty quantification of the speed made good was conducted. Realizations from the distributions were generated and evaluated using the DKG models to generate speed made good realizations, i.e., the speed made good distribution. The distribution of the speed made good was calculated for each cell in the raster defining the KRC area for the CDT event. Using the speed made good distributions, the stochastic speed made good maps were generated.

The 90%, 50%, 10% stochastic maps and deterministic maps are shown in Fig. 10 and Fig. 11 for simple and complex terramechanics, respectively. The deterministic map is the map generated if no variability is considered and deterministic values of the soil parameters, typically mean values, are used. The deterministic slope used is calculated from the measured elevation values and does not consider any variability in the elevation or slope. The 90% speed made good map means there is 90% probability that the maximum obtainable speed is greater than or equal to the speed shown in the map. As you decrease the probability level, for example going from 90% to 50%, the speed in the map will increase. This means the speed shown the 50% map is going to higher than the speed shown in the 90%, however, there is only 50% probability of actually obtaining the speed shown in the 50% map.

Studying the loop in the lower righthand corner of the speed made good maps shown in Fig. 10, we can see how the speed in the map changes depending on if you are looking at the 90%, 50%, 10%, or deterministic map. In the 90% map the speed on the loop looks to range between 30-40 km/h, in the 50% map the speed on the loop looks to range between 60-70 km/h, in the 10% map the speed on the loop looks to range between 110-130 km/h, and in the deterministic map the speed looks to range between 110-130 km/h. Thus, it looks like there is only about 10% probability of obtaining the speed shown in the deterministic map for that loop. Other areas of the deterministic map look to have different probabilities of obtaining the speed shown. For example, the green circle areas on the left side of the maps look to be green in the 90%, 50%, 10%, and deterministic map. Therefore, there is about 90% probability of obtaining the speed shown in the deterministic map for those circle areas. This shows that deterministic map may not be reliable in providing the actual speed made good. This is further illustrated in Fig. 12, which shows the simple terramechanics deterministic speed made good (top map) and corresponding probability level maps (bottom map). The probability level map shows the probability of obtaining the speed value shown in the deterministic speed made good map. As seen in the probability map, the probability ranges from 0-90%, thus, the speed made good values provided by deterministic map are not reliable.

It is interesting to compare the speed made good maps obtained using the simple terramechanics as shown in Fig. 10 to those obtained using the complex terramechanics as shown in Fig. 11. The maps show similar patterns, the higher speed areas agree between the two, however, the actual speed value does not agree well. For example, the speed of the circle areas on the left side of the 90% simple terramechanics map ranges between 110-130 km/h, while for the same area in the complex terramechanics map the speed ranges between 60-70 km/h. The speed range for this area for the simple terramechanics is almost double that of the complex terramechanics for the same area.

This raises the question why the two different maps do not agree with each other. There is a long list of possibilities. Maybe one of the two models does not predict correctly, maybe the distributions used for the soil parameters do not capture the true distribution very well, etc. This leaves room for future work

to be carried out to study the differences between the simple and complex terramechanics models, the soil parameters used in both, the need for more soil data and better identification of the distribution and correlation for the soil data.

The large patterns of the speed for both simple and complex terramechanics look to correspond to the soil type. This can be seen by comparing the speed made good maps in Fig. 10 and Fig. 11 to the soil type map shown in Fig. 13. For example in Fig. 13 the peat soil type is shown as the purple color, this purple area is similar to the lowest speed areas, i.e., reddish colored areas in the speed made good maps shown in Fig. 10 and Fig. 11. Thus, one general conclusion might be that when on peat soil the speed will be lower. This shows that knowing the correct soil type as well as having enough data to identify the correct distributions and correlation of the soil parameters is critical for obtaining accurate stochastic speed made good maps. This is also explaining why even in the stochastic speed made good maps there is little variability in the speed for large areas in the map.

One possible use of the speed made good map is for path planning in order to find the optimal route for getting from point A to point B. Fig. 14 below shows the optimal path between two points for the 90%, 50%, 10%, and deterministic maps. The path provided by the deterministic map is the path when no variability is taken into consideration. The path provided by 90% map, gives the path that has 90% probability of obtaining the speed given by the 90% speed made good map, along the path. Likewise, the path provided by 50% and 10% maps have 50% and 10% probability of obtaining the speed along the path, respectively. Comparing the different paths, it is easily seen that the 90% and deterministic paths are different with just a few segments that are the same along the paths. The paths provided by the 50% and 10% look to more closely match that of the path given by the deterministic map. The 90% path is a more conservative path because there is 90% probability of obtaining the speed along the path. Therefore, the 90% path will most likely not be the fastest path as seen in Fig. 14. However, one interesting point is that, the 90% path in this case is a shorter distance path at 1.58 km than the deterministic path at 1.63 km. Fig. 15 shows the 90% path compared to the deterministic map with the probability of some segments of the deterministic path labeled. This figure clearly shows how the deterministic path is not a reliable path, some segments of the path only have 0-10% probability of obtaining the speed along the path, while another segment has 40-50% and another 80-90% probability of obtaining the speed along the path. Thus, if the deterministic path is used, the probability of being able to make it from point A to point B is unknown, if it is even possible to make it between the two points and the predicted time is most likely inaccurate. Thus, for missioning planning the stochastic mobility maps provide valuable information to the decision maker planning the path, leading to increased mission success.

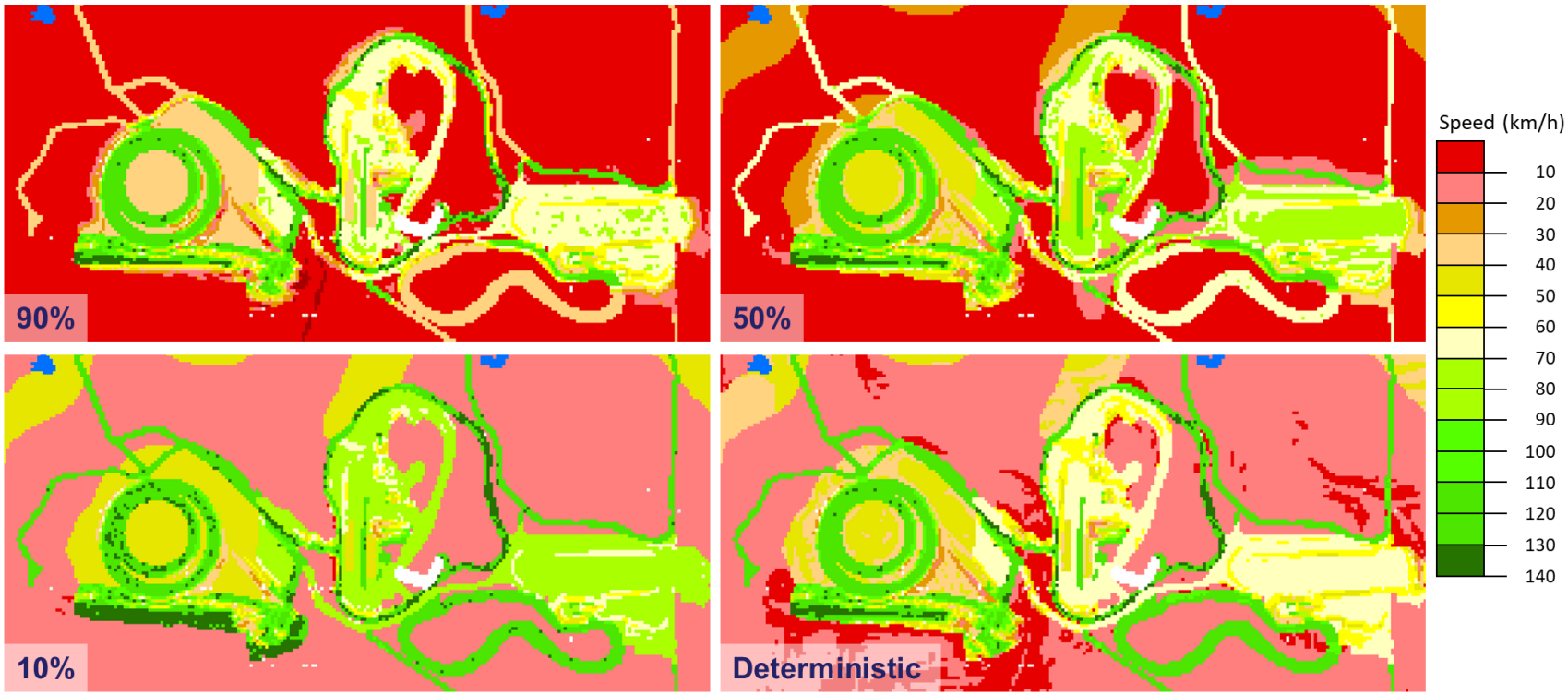

Fig. 10: Simple Terramechanics Speed Made Good Maps

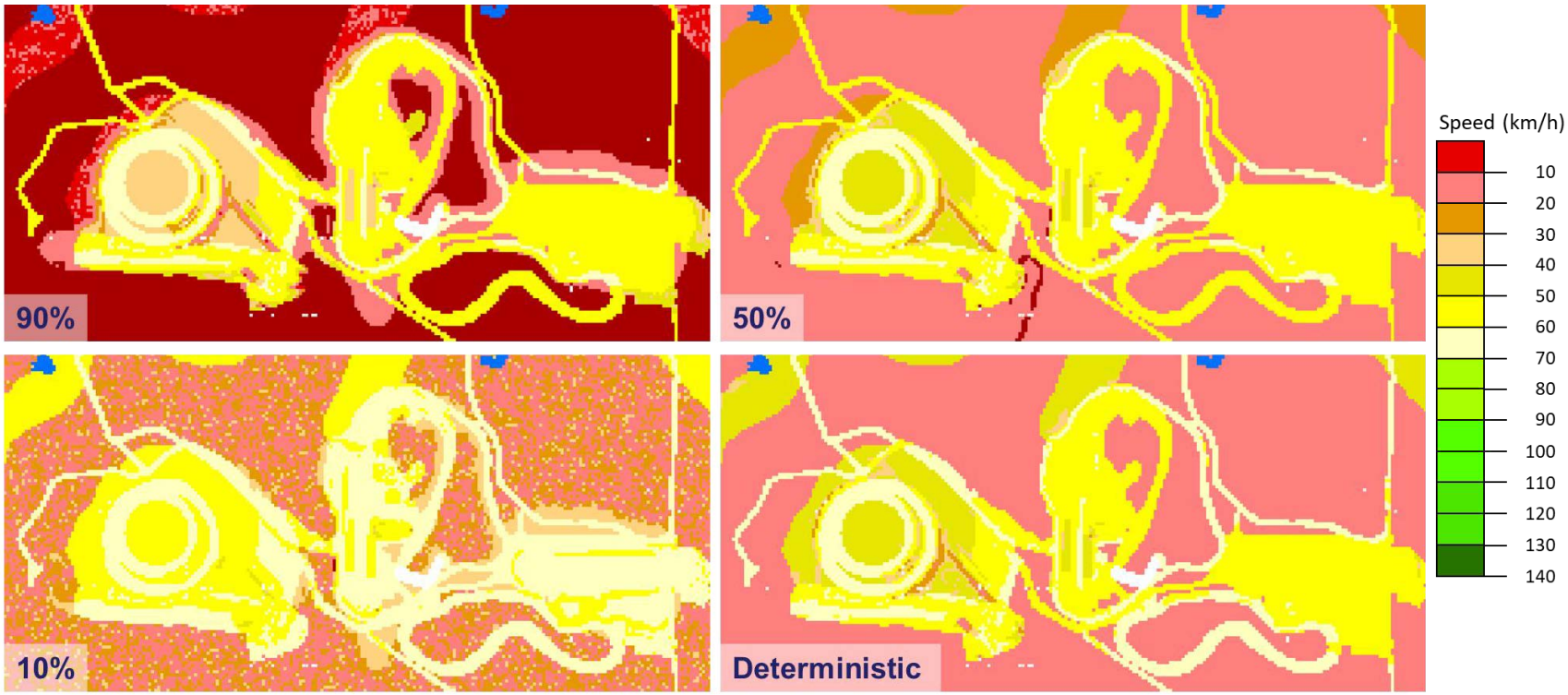

Fig. 11: Complex Terramechanics Speed Made Good Maps

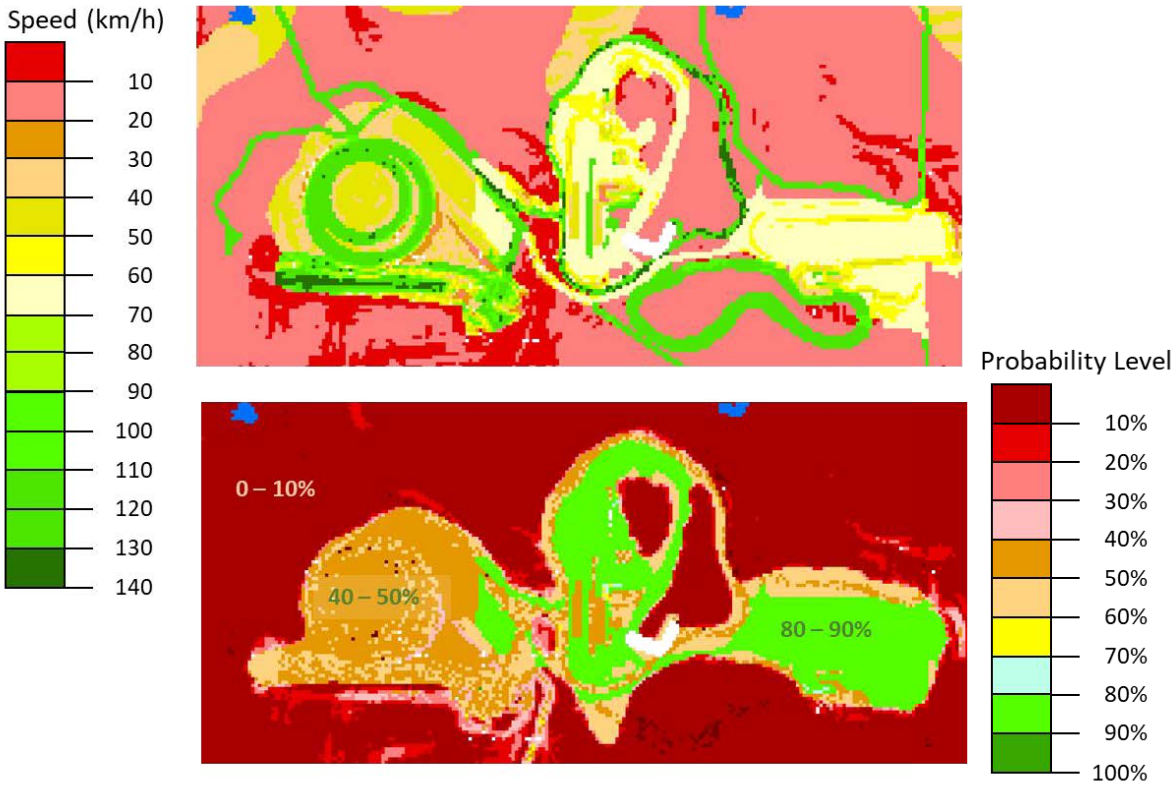

Fig. 12: Simple Terramechanics Deterministic Speed Made Good and Corresponding Probability Level

Fig. 13: Soil Type

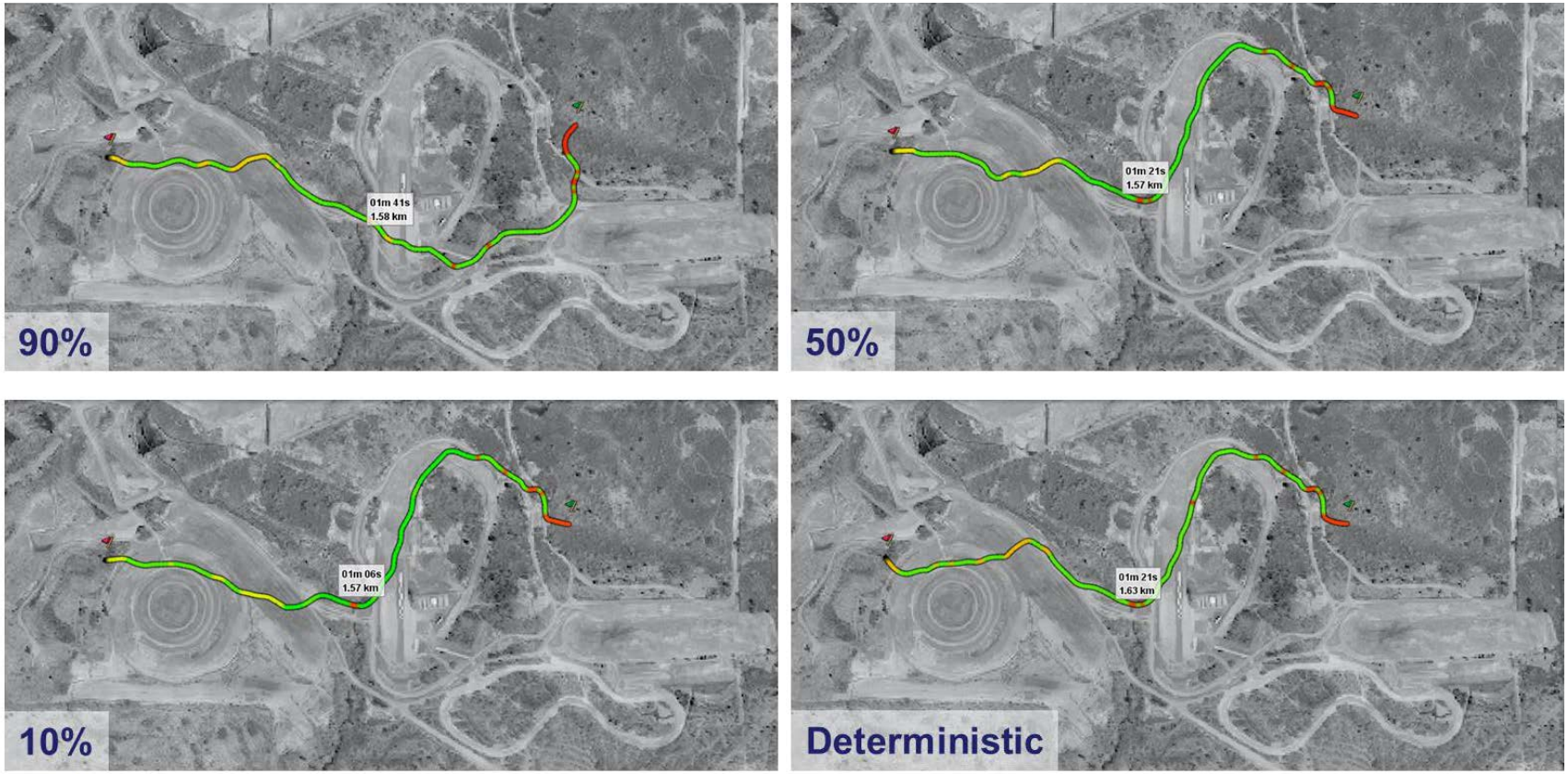

Fig. 14: Path Planning Maps

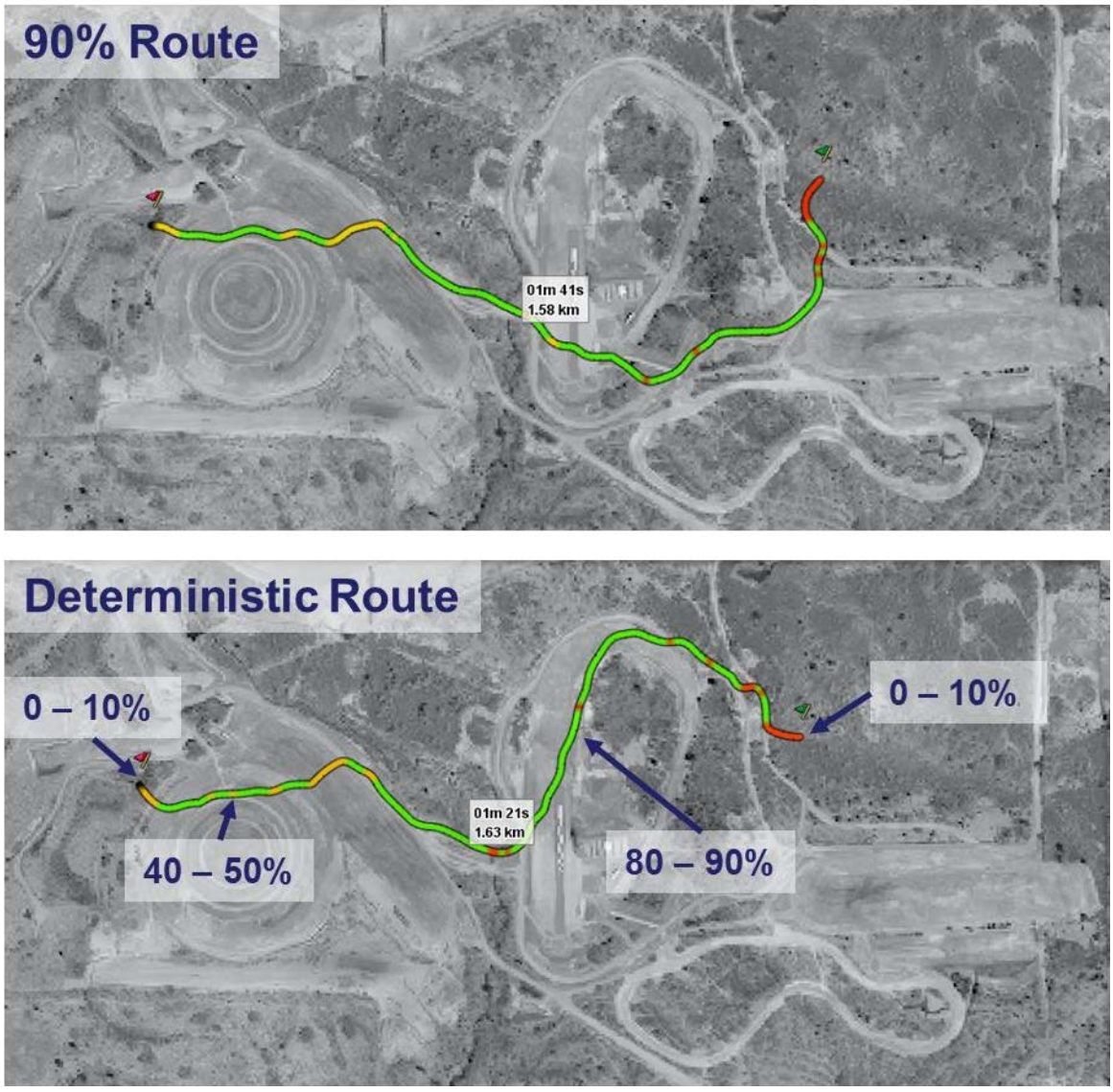

Fig. 15: Deterministic Path and Probability Compared to 90% Path

Summary and Conclusion

In summary the data collected by KRC for the CDT event was used together with data from Ref. [8] to assemble a larger data set. This larger data set was used to determine the distributions that best fit the data and the stastical correlation between Keq and n. The DOE points needed to fit the dynamic Kriging (DKG) model were generated using RAMDO software and evaluated by the vendors. The DKG model was then used in RAMDO for carrying the uncertainty quantification of the speed made good. In comparing the stochastic maps given by simple and complex terramechanics they were notably different. This leaves room for future to determine why this may be. The stochastic mobility maps were generated, and path planning routes created for them. It was shown how the 90% and deterministic paths were different and how the deterministic path is not a reliable path, with segments of it having 0-10% probability of obtaining the speed provided in the deterministic map. Thus, the stochastic maps provide

valuable information to the decision makers planning paths or other operations for increasing mission success.

References

[1] McCullough, M., Jayakumar, P., Dasch, J. and Gorsich, D. (2016). Developing the Next Generation NATO Reference Mobility Model. 2016 Ground Vehicle Systems Engineering and Technology Symposium (GVSETS), August 2-4, Novi, MI.

[2] Rula, A.A. and Nuttall, C.J. (1971). An Analysis of Ground Mobility Models (ANAMOB). Tech. Report M-71-4. US Army WES, Vicksburg, Mississippi.

[3] Haley, P.W., Jurkat, M.P. and Brady, P.M. (1979). NATO Reference Mobility Model, Edition I. Tech. Report 12503. US Army TARDEC, Warren, Michigan.

[4] Lessem, A., Ahlvin, R., Mason, G., and Mlakar, P. (1992). Stochastic Vehicle Mobility Forecasts Using the NATO Reference Mobility Model - Report I: Basic Concepts and Procedures. Technical Report GL-92-11. US Army TARDEC, Warren, Michigan.

[5] Lessem, A., Ahlvin, R., Mlakar, P., and Stough, W. (1993). Stochastic Vehicle Mobility Forecasts Using the NATO Reference Mobility Model - Report II: Extension of Procedures and Application to Historic Studies. Technical Report GL-93-15. US Army TARDEC, Warren, Michigan.

[6] Lessem, A., Mason, G. and Ahlvin, R. (1996). Stochastic vehicle mobility forecasts using the NRMM. Journal of Terramechanics, 33(6): 273-280.

[7] Vong, T., Haas, G. and Henry, C. (1999). NATO Reference Mobility Model (NRMM) Modeling of the DEMO III Experimental Unmanned Ground Vehicle (XUV). ARL-MR-435, Army Research Laboratory, Aberdeen Proving Ground, Maryland.

[8] Wong, J Y (Jo Yung). 2010. Terramechanics and Off-Road Vehicle Engineering Terrain Behaviour, off-Road Vehicle Performance and Design / J.Y. Wong. 2nd ed.. Oxford: Oxford : Butterworth-Heinemann.